Research Article

Theoretical formulations and simulations of one-dimensional inhibition kinetics of ethanologenic microorganisms in batch fermenters

Peter P. Bamaalabong[1,2] · Nana Y. Asiedu[2] · F. Abunde Neba[3] · Francesca Baidoo[2] · Ahmad Addo[4]

Received: 16 August 2020 / Accepted: 16 August 2021
Published online: 26 August 2021

Abstract

The utilization of bio-based technology for energy has piqued researchers' curiosity around the world. As a result, bioethanol fermentation has been a hot topic of research for many scientists since it uses less energy and chemicals, produces fewer harmful by-products and emissions, and has environmentally favorable applications. The modeling and simulations of one-dimensional product and substrate inhibitions for sorghum, maize, and cassava extracts are discussed in this paper. Because it provides an edge over other methodologies, mechanistic modeling techniques are used. Models of substrate and product inhibitions in one dimension (1-D) are constructed. These 1-D models are then confirmed using parameter estimates before being employed in the work's simulations. For each dynamic model constructed, model fitness coefficients (α) are calculated. For the product, the exponential inhibition model, sorghum extract data has the best model fitness coefficient (α = 0.4088), for product sudden stop inhibition model and cassava extract data gives the best model fitness coefficient ($\alpha = 0.4417$) for product exponential model. The projected yield increases for substrate exponential inhibition with sorghum extract data, substrate linear inhibition with maize extract data, and substrate linear inhibition with cassava extract data are 74%, 27%, and 25%, respectively. This unique framework has offered the industry a wide choice of kinetics models to choose from to alleviate inhibitions in fermentation systems and maximize yield and productivity in the bioethanol fermentation process.

Article Highlights

- The modeling of inhibitions namely linear, sudden stop, and exponential in batch fermentation processes are presented in this article.
- Model fitness coefficient analysis showed the product as a primary inhibitor and substrate as a secondary inhibitor during the process
- The cassava and maize processes described linear inhibition model and sorghum fermentation showed exponential product inhibition model.

Keywords Inhibitions · Fermentation · Kinetic modelling · Simulations · Batch fermenter · Ethanologenic microorganisms · Wort

✉ Nana Y. Asiedu, nasiedusoe@yahoo.co.uk | [1]Department of Anesthesia and Intensive Care, School of Medicine and Health Science, University for Development Studies, Tamale, Ghana. [2]Department of Chemical Engineering, Faculty of Mechanical and Chemical Engineering, College of Engineering, Kwame Nkrumah University of Science and Technology, Kumasi, Ghana. [3]Department of Civil and Environmental Engineering, Norwegian University of Science and Technology, Trondheim, Norway. [4]Department of Agricultural and Biosystems Engineering, Faculty of Mechanical and Chemical Engineering, College of Engineering, Kwame Nkrumah University of Science and Technology, Kumasi, Ghana.

1 Introduction

For both industrial and domestic consumption, the global economy is heavily reliant on energy sources. Despite this reliance, there is a growing global interest in using bio-based technologies for energy generation because fossil fuel supplies are finite and their extraction results in high greenhouse gas emissions, according to Vohra et al. [1]. Because it is recognized as an efficient and sustainable alternative in the provision of a considerable amount of energy that helps sustain energy supply to our society, bioenergy, which is eco-friendly, is steadily and widely adopted in the energy business, according to Choi et al. [2]. Bioethanol fermentation has piqued researchers' interest among the various bioenergy generation techniques since it consumes less energy during the fermentation process, produces less harmful by-products and emissions, and its uses are environmentally favorable, Pulidindi et al. [3]. Bioethanol fermentation is a rapidly increasing application that has been researched by researchers in the food and beverage sectors Marshal et al. [4]. Other applications include medicine, cosmetics, and pharmaceuticals for antiseptic, disinfection, and antidote, Harde et al. [4], Pulidindi et al. [3]. Bioethanol fermentation for the manufacture of the first-generation, second-generation, and third-generation biofuels using simple sugars, starch, lignocellulosic, and seaweed has recently become the focus of research Chisti [5]. The project fosters reduced rivalry for fossil fuel deposits and arable land, which are scarce. Since it has been demonstrated that 0.3934 kg of galactose can be produced from 1 kg of seaweed (Eucheuma), and 1.18 kg of seaweed can be obtained from one square meter of annual cultivation, seaweed has been investigated as a natural resource with the potential to be developed as a raw material for bioethanol Goh et al. [6], however, due to the impact of inhibitors on the substrate in the form of toxic chemicals and the limited ability of bacteria to ferment galactose, fermentation approaches for the manufacture of bioethanol from seaweed are still inefficient Alriksson [7]. The fermenter is the most important element in the bioethanol fermentation process, and appropriate environmental conditions are necessary to generate the desired output Alford [8]. The utilization of bioreactors for commercial-scale production often comes with operational issues, such as dealing with inhibitors Asiedu et al. [9], Han [10]. This has a detrimental impact on bioethanol yield and productivity. Several techniques have been employed to reduce substrate inhibitions in bioreactors during bioethanol fermentation. Genetic approaches, which require specialized laboratory procedures, are blind to complex research such as metabolic pathways which are difficult to comprehend Palsson et al. [11], Brenner [12]. Due to the vast amount of data involved, statistical design of experiments, which is limited by dimensional space due to the cost and time of numerous experimental rounds, has been the problem of local optima and low-speed computing sequences Schoneberger et al. [13], Boer et al. [14]. Mechanistic modeling of biochemical kinetics is a conceptual problem-solving approach Yu et al. [16]. This method uses quick simulation sequences that can be used for global optimization problems Ming et al. [15]. An important accomplishment in improving the efficiency of bioethanol fermentation, which translates to greater yield and productivity, is obtaining a more dependable and robust technique for reducing the problems of inhibitions. Although research on mathematical modeling and simulation to describe substrate and product inhibitions in fermenters has been conducted, it should be noted that not all degrees of freedom of the problem are considered at the same time. Abunde et al. [16], for example, modeled one-dimensional product inhibition in sorghum and maize. Asiedu et al. [9] looked at a two-dimensional product and substrate inhibition for cassava in another investigation. Thus, for sorghum, maize, and cassava extracts, this research proposed a general modeling technique for 1D product and substrate inhibitions. Mechanistic modeling techniques were used in the study, which has an advantage over other methodologies Harmelen et al. [19]. The research was divided into two sections: Mathematical modeling was used to generate one-dimensional substrate and product inhibition models through a combination of the Monod equation and inhibition models to generate inhibition patterns. These models were then validated using data generated from some breweries in Ghana. The paper is therefore arranged as follows:

The Abstract Comprises a motivation statement, objectives of the work, materials and methods used, results obtained after the analysis, conclusion, and key findings of the work. Section 1 consists of an introduction and a brief literature review, importance of the work, problem statement, controversies if any, justification or unique solution, objective, and method of the study. Section 2 describes the approaches and methods. The relevant theoretical development behind the modeling of the types of inhibitions that occur during fermentation is extensively reviewed. Section 3 described parameter estimations determination of the derived inhibition models. In Sect. 4, a generalized framework for modeling one dimension product and one dimension substrate inhibitions models was formulated. The fermenter dynamic models derived were fitted to Monod kinetics and all constants were

determined. In Sect. 5 the calculations of the model fitness coefficient were determined to ascertain the robustness of the models used in the work. Section 6 discusses the visualization effect and increase in yield. In Sect. 7 of the work, a control strategy for the types of inhibitions studied was proposed. Section 8 discusses the results of the study and the presentation of the main findings of the work. Section 9 thus concludes this research study through remarkable comments along with future useful works.

2 Theoretical developments

2.1 Substrate and product inhibitions modeling

The effect of inhibitions modeling on the specific growth rate of ethanologenic bacteria is shown in Fig. 1a and b. The specific growth rate increases as the substrate concentration increase until the optimum specific growth rate is reached at a particular concentration. As shown in Fig. 1a, the specific growth rate begins to decline at this concentration. This is due to the fermentable sugars exerting significant osmotic pressure on the ethanologenic bacteria. Increased product concentration does not appear to boost the specific growth rate. Any rise in product concentration (inhibitory concentration) in the fermenter results in a decreased specific growth rate as shown in Fig. 1b. The alcoholic stress on the yeast cells causes the drop in specific growth rate. In bioreactors, inhibition can be defined as a material that harms yeast cells without killing them, however, if the inhibitory substance causes cell death, it is classified as a toxic substance Kristensen [17], Kaparuju [18].

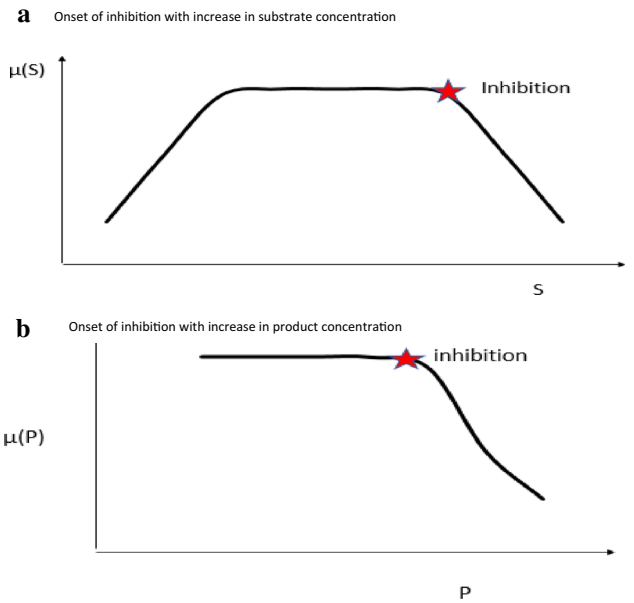

Fig. 1 **a** The Onset of substrate inhibition, **b** The Onset of product inhibition

The kinetics of cell growth is heavily influenced by the cell's physiology, nutritional requirements, and sensitivity to external circumstances, Basso et al. [19]. The yeast strains employed during the fermentation process are (a) Ale yeasts, (b) Lager yeasts, and (c) Wild yeasts. As a result of environmental variables, product and substrate inhibitions, the yeast cells stated have varied properties. It is shown that the nature of fermentable sugars obtained from different carbohydrate sources differs, in terms of their growth kinetics and hence response pattern to inhibitions of a given microorganism. In this study, three types of inhibition patterns will be considered: linear, exponential, and sudden stop, as shown in Fig. 2.

According to research to the inhibition of substrate and product on microbial cells is based on very similar effects and is tightly linked, Stambaugh [20]. The three inhibition patterns given in Table 1 describe how fermentation yeasts respond to inhibition. The mathematical formulas for the three inhibition patterns for both substrate and product are shown in Table 1.

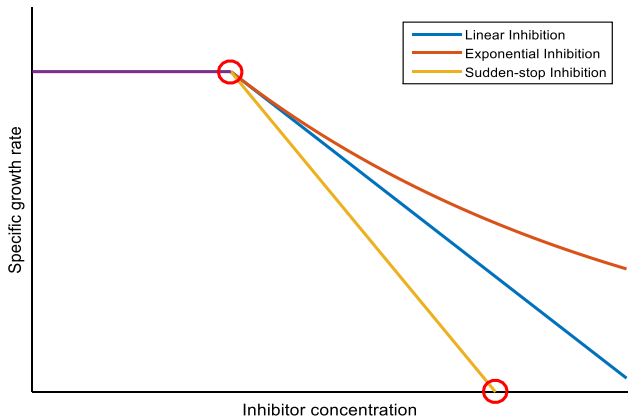

Fig. 2 Patterns of substrate and product inhibitions on microbial growth

Table 1 Mathematical expressions for Substrate and Product inhibitions patterns *Source* Abunde, Asiedu et al. [18]

SN	Inhibition patterns	Mathematical expressions	
		Substrate	Product
1	Linear	$(1 - K_{iS}S)$	$(1 - K_{iP}P)$
2	Sudden stop	$\left(1 - \frac{S}{S_{max}}\right)$	$\left(1 - \frac{P}{P_{max}}\right)$
3	Exponential	$\exp(-K_{iS}S)$	$\exp(-K_{iP}P)$

2.2 Geometries of one-dimensional inhibition

The Monod function, Eq. (1), is commonly used to model microorganisms' growth rate. For this investigation, Monod [21] was used.

$$\mu = \mu_m \frac{S}{K_s + S} \tag{1}$$

where μ_m is the maximum specific growth rate (hr^{-1}) and K_S is the Monod constant (g/L).

The effects of substrate and product inhibitions on cell growth are assumed to be one-dimensional, with cell growth reduction attributed to either substrate or product inhibition. Modifying Eq. (1) above with the three possible inhibition patterns for substrate and product models yielded one-dimensional substrate, inhibition models. Modifying the Monod growth function with the three possible product inhibition patterns yielded one-dimensional product, inhibition models.

Figure 3 shows how these developments were made by non-convoluted recombination of the substrate or product with the inhibitory patterns.

The derived one-dimensional models-substrate inhibitions- are presented by Eqs. (2), (3), and (4)

$$\mu(S) = \frac{\mu_{max} S}{K_s + S}(1 - K_{is} S) \tag{2}$$

$$\mu(S) = \frac{\mu_{max} S}{K_s + S} e^{-K_{is} S} \tag{3}$$

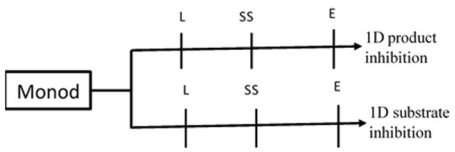

Fig. 3 Modifying Monod growth function with three possible inhibition patterns

$$\mu(S) = \frac{\mu_{max} S}{K_s + S}\left(1 - \frac{S}{K_{is}}\right) \tag{4}$$

where $K_{is} and \left(S_{max}\right)^{-1}$ (Table 2) are the initial values of inhibitor's concentration that does not bring about the incidence of toxicity in the fermenter.

On the other hand, the one-dimensional product inhibition models are presented by Eqs. (5), (6), and (7)

$$\mu(S,\ P) = \frac{\mu_{max} S}{K_s + S}(1 - K_{ip} P) \tag{5}$$

Hinshelwood– Dagley [22]

$$\mu(S, P) = \frac{\mu_{max} S}{K_s + S} e^{-K_{ip} P} \tag{6}$$

Aiba and Shoda [23]

$$\mu(S, P) = \frac{\mu_{max} S}{K_s + S}\left(1 - \frac{P}{K_{ip}}\right) \tag{7}$$

Ghose and Tyagi [24]where $K_{is} and \left(P_{max}\right)^{-1}$ are final values of the inhibitor's concentration that does not bring about the incidence of toxicity in the fermenter.

The list of model parameters to be determined is presented in Table 2.

2.3 Models that describe the fermentation process dynamically

The biochemical processes explain the fermenter's biological and chemical reactions. It is taken into accounts the mathematical advances that depict the biochemical activities that occur in the fermenter. The following three different inhibition models are considered in this scheme Bastin and Dochain [28]

a) The reaction is assumed a pure chemical reaction and no biomass is involved:

$$S_1 + S_2 + \ldots + S_n \rightarrow P_1 + P_2 + \ldots + P_m \tag{8}$$

Table 2 List of model parameters

SN	Parameter	Description	Units
1	μ_{max}	Maximum specific growth rate	h^{-1}
2	K_{is}	Substrate inhibition coefficient on cell growth	g/l
3	K_{ip}	Product inhibition coefficient on cell growth	g/l
4	K_s	Substrate saturation (Monod) constant for cell growth	g/l
5	Y_{PS}	Yield coefficient of product based on substrate utilization	g/g
6	Y_{XS}	Yield coefficient of cell-based on substrate utilization	g/g
7	G_s	The specific rate of substrate consumption for cell growth	g/(g.h)
8	M_s	The specific rate of substrate consumption for cell maintenance	g/(g.h)

The biomass (X) is assumed to be used by the enzyme associated with the reaction since is not isolated from the yeast:

$$S_1 + S_2 + \ldots + S_n \rightarrow^{X} P_1 + P_2 + \ldots + P_m \quad (9)$$

b) The reaction is associated with the growth of microorganisms which therefore makes biomass a product is given below:

$$S_1 + S_2 + \ldots + S_n \rightarrow^{X} P_1 + P_2 + \ldots + P_m + X \quad (10a)$$

c) The production of ethanol by yeast is a result of the yeast consuming sugars as an energy source for cell growth. This process thus results in Eq. 10(b).

$$S \rightarrow^{X} P + X \quad (10b)$$

The production of ethanol by yeast is a result of the yeast consuming sugars as an energy source for cell growth. This process thus results in Eq. 10(b).

The species conservation equations for the batch ethanol fermentation process can be presented as follows: Eqs. (11) to (13).

Biomass mass balance in the fermenter (X)

$$\frac{dX}{dt} = r_X = \mu X \quad (11)$$

Product mass balance in the fermenter (P)

$$\frac{dP}{dt} = r_P = Y_{PX}\mu X \quad (12)$$

Substrate mass balance in the fermenter (S)

$$\frac{dS}{dt} = r_S = -\frac{1}{Y_{XS}} r_X - \frac{1}{Y_{PS}} r_P - M_s X \quad (13)$$

Where $Y_{PS} = Y_{XS} \times Y_{PX}$.

2.4 Estimation of parameters

Factors to consider when estimating parameters:

The fermenter model was developed using several considerations to analyze the process data. This entails calculating the model parameters using industrial process data and then assessing the feed stock's quality using statistical methodologies. The analysis employed to process data for the fermentation of Sorghum, Maize, and Cassava Extracts, and the criterion used to fit the model is shown in Eq. (14)

$$S(k) = \sum_{i=1}^{n} \left[y_i - \hat{y}(t_i, k)\right]^T W_i \left[y_i - \hat{y}(t_i, k)\right] \quad (14)$$

where $\boldsymbol{y_i}$ is a two-dimensional vector of response values at a time $\boldsymbol{t_i}$ and $\boldsymbol{W_i}$ are 3×3 weight matrices for each observation point $\boldsymbol{i}$. $\hat{\boldsymbol{y}}(\boldsymbol{t_i}, \boldsymbol{k})$ is the predicted response value at a time $\boldsymbol{t_i}$ and its relation to the bioreactor model solution is given by Eq. (15). Equation (16) represents the three-dimensional solutions of the bioreactor model used for the fermentation.

$$\hat{y}(t_i, k) = C.x(t_i, k) + \varepsilon \quad (15)$$

where

$$x(t_i, k) = [X(t), P(t), S(t)]^T \quad (16)$$

and

$$C = \begin{pmatrix} 0 & 1 & 0 \\ 0 & 0 & 1 \end{pmatrix}$$

C represents a 2×3 matrix indicating the state variables that were measured.

The model equations were numerically integrated using the Runge–Kutta 4-5th order method, which was implemented by the ode45 procedure, and the minimization issue was addressed using the interior point algorithm of the fmincon routine, using the Matlab optimization toolbox.

2.5 Assessing quality of parameter estimates

A linearization approach was used to examine the parameter estimates' variability. Equation (16) was used to calculate the noise variance of the parameter estimations, and Eq. (17) was used to approximate the covariance matrix (17)

$$\sigma^2 = \frac{1}{n-p} \sum_{i=1}^{n} \left(y_i - \hat{y}(t_i, k)\right)^2 \quad (17)$$

$$cov(k) = 2\hat{H}^{-1}\sigma^2 \quad (18)$$

The standard error of the parameter estimates ($s_{\hat{\beta}_i}$) is given by Eq. (18). The correlation matrix is computed using Eq. (19) and the coefficients of variation.

were obtained by using Eq. (20).

$$s_{\hat{k}_i} = \sqrt{diag\left(cov\left(\hat{k}\right)\right)} \quad (19)$$

$$corr\left(\hat{k}\right) = \frac{cov_{i,j}}{\sqrt{cov_{i,i}}\sqrt{cov_{i,j}}} \quad (20)$$

$$CV = \frac{\sqrt{diag\left(cov\left(\hat{k}\right)\right)}}{\hat{k}_i} \quad (21)$$

By inputting the process data, the software performed an automated fitting for 19 models and ranks them in order of best fit using both numerical and graphical approaches. The numerical approach resides in the computation of a parameter referred to as alpha (*α);* the model fitness coefficient (Eq. 21), which takes into account four statistical coefficients for its computation. These coefficients, which included, the coefficient of determination (R^2), adjusted coefficient of determination (R^2Adj), root mean square error (*RMSE*) and the reduced chi-square (χ^2) were major validation criteria for model selection. The criteria for a good quality fit is that R^2, and R^2Adj values are high while *RMSE* and χ^2 are low, Hahn [25], Huang [26], Cameron [27].

$$\alpha = \chi^2 + \text{RMSE} + \left(1 - \text{R}^2\text{Adj}\right) + \left(1 - \text{R}^2\right) \quad (21)$$

If models have a similar correlation coefficient, models with the lowest values are deemed appropriate to represent a specific data set. The contours that describe the correlation between the model parameters are examined using the graphical technique.

3 Dynamic models

A generic framework for modeling one-dimensional product and substrate inhibitions was developed from sorghum, maize, and cassava extracts data. Because of its great accuracy for pure cultures and simple substrates, the Monod model was chosen as the foundation for modeling the inhibitions, Contois [28]. More so, the Monod model is very suitable for homogenous cultures with similar characteristics Boekhorst et al. [29] and cannot competently describe the degradation of a complex substrate such as urban waste Pfeffer [30]. Within the context of one dimension inhibition modeling, product or substrate inhibitions were appropriate to our study. Three (3) inhibition patterns, namely linear, exponential, and sudden halt, were evaluated, as well as three sets of data from three different substrates, namely sorghum, maize, and cassava. In total, 19 fermenter bioreactor models were developed and validated using parameter estimation for their respective kinetic constants, model fitting of their respective substrate use, and product formation curves concerning process data. Model fitting for substrate sudden stop inhibition using cassava extract data and product sudden stop inhibition using sorghum extract data did not converge, hence they were removed from the study. For best-performing models selection, the quality of parameters estimated was tested using a linearization to produce the model fitness coefficient (α). (Eq. 21).

3.1 Fermenter dynamic models fitting with monod kinetics

Figure 4 shows the process data for sorghum, maize, and cassava extracts after fitting the Monod-based dynamic model. Table 3 shows the estimated kinetic constants and statistical validation parameters used to test the fitting quality, revealing that the sorghum extract (Fig. 4a) has a very high R^2 (0.9947) and a low RMSE (0.0923). R^2 is high (0.870) for maize extract (Fig. 4b), and, X^2 *(77.239)* remains high as well.

Similarly, the cassava extract (Fig. 4c) has a high value of R^2. (0.7736) and a moderate value of, X^2 (20.9467).

3.2 One-dimensional substrate inhibition

Model fitting of a one-dimensional substrate linear inhibition dynamic model with data from sorghum, maize, and cassava extracts is shown in Fig. 5. Table 4 shows the calculated kinetic constants and statistical validation values for evaluating the quality of model fitting. With sorghum extract data (Fig. 5a), the one-dimensional substrate linear inhibition dynamic model has a very low R^2 (0.3110) value and a very high X^2 (576.5204) value. With maize extract data (Fig. 5b), the linear inhibition dynamic model has a very low value of R^2 (-0.621) and a very high value of X^2 (1880.440). The R^2 value of the same inhibition dynamic model fitted to cassava extract data (Fig. 5c) is very low R^2 (-1.3895), whereas the value of X^2 is very high.

With data from sorghum, maize, and cassava extracts, Fig. 6 shows a model fitting of one-dimensional substrate exponential inhibition dynamics. Table 5 shows the estimated kinetic constants as well as statistical validation results.

Model fitting of one-dimensional substrate exponential inhibition dynamics with sorghum extract data (Fig. 6a) shows a very high R^2 (0.9945) value and a very low RMSE value (0.0956). The one-dimensional substrate exponential inhibition dynamics model fitting using maize extract data (Fig. 6b) has a high R^2 (0.856) value and a very high X^2 value (117.238). The same inhibition dynamic model fitted to cassava extract data (Fig. 6c), has a moderate value of R^2 (0.7516) and a moderate value of χ^2 (25.0265).

Figure 7 illustrates the experimental data for sorghum, and maize extracts with a model fitting of one-dimensional substrate sudden halt inhibition dynamics. The computed kinetic constants and statistical validation parameters are listed in Table 6. The model fitting of one-dimensional substrate sudden stop inhibition dynamics with sorghum

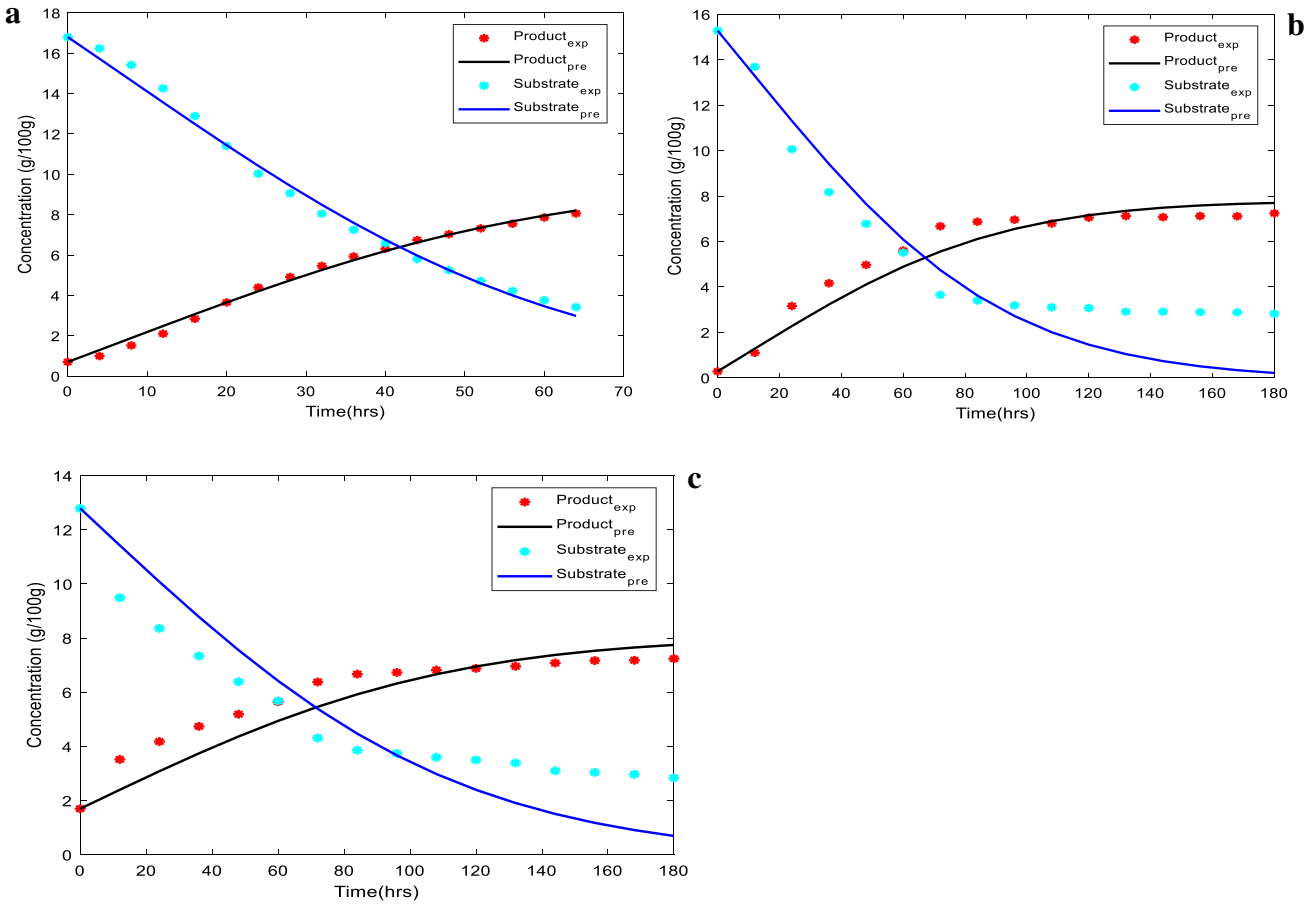

Fig. 4 Model fitting using Monod kinetics without inhibition for fermentation of Sorghum (**a**), Maize (**b**), and Cassava (**c**) extracts

Table 3 Estimation of kinetic constants and statistical validation for Monod model

Models	Parameter estimates						Statistical validations		
	μ_{max}	K_s	Y_{PX}	Y_{XS}	M_s	K_{iS}	*RMSE*	χ^2	R^2
Batch 1: Sorghum extracts									
Monod	0.0608	49.999	19.2230	0.0301	0.0100	5.0058	0.0923	0.5430	0.9947
Batch 2: Maize extracts									
Monod	0.044	50.000	50.000	0.010	0.010	5.001	1.334	77.239	0.870
Batch 3: Cassava extracts									
Monod	0.0358	50.0000	50.0000	0.0105	0.0100	4.9999	1.1826	20.9467	0.7736

extract data (Fig. 7a) has a very low,R^2 (0.3110) and a very high X^2 (576.5204). Model fitting of the same abrupt halt inhibition dynamics with maize extract data (Fig. 7b), on the other hand, shows a very low value of R^2 (-1.055) and a very high value of X^2 (1869.142).

3.3 One-dimensional product inhibition

With data from sorghum, maize, and cassava extracts, Fig. 8 shows the model fitting of product linear inhibition dynamics. Table 7 shows the calculated statistical validation results and predicted kinetic constants. Model fitting of product linear inhibition dynamics with sorghum (Fig. 8a) revealed a high R^2 (0.9944) value and a low RMSE value (0.0980). Model fitting of the product linear inhibition dynamics with maize extract data (Fig. 8b) exhibited a high R^2 (0.9850) value. The same inhibitory dynamic model (Fig. 8c) obtained a very high R^2 (0.9794) value when fitted to cassava extract data.

With data from sorghum, maize, and cassava extracts, Fig. 9 displays a model fitting of an exponential inhibition dynamic model. Table 8 shows the estimated kinetic

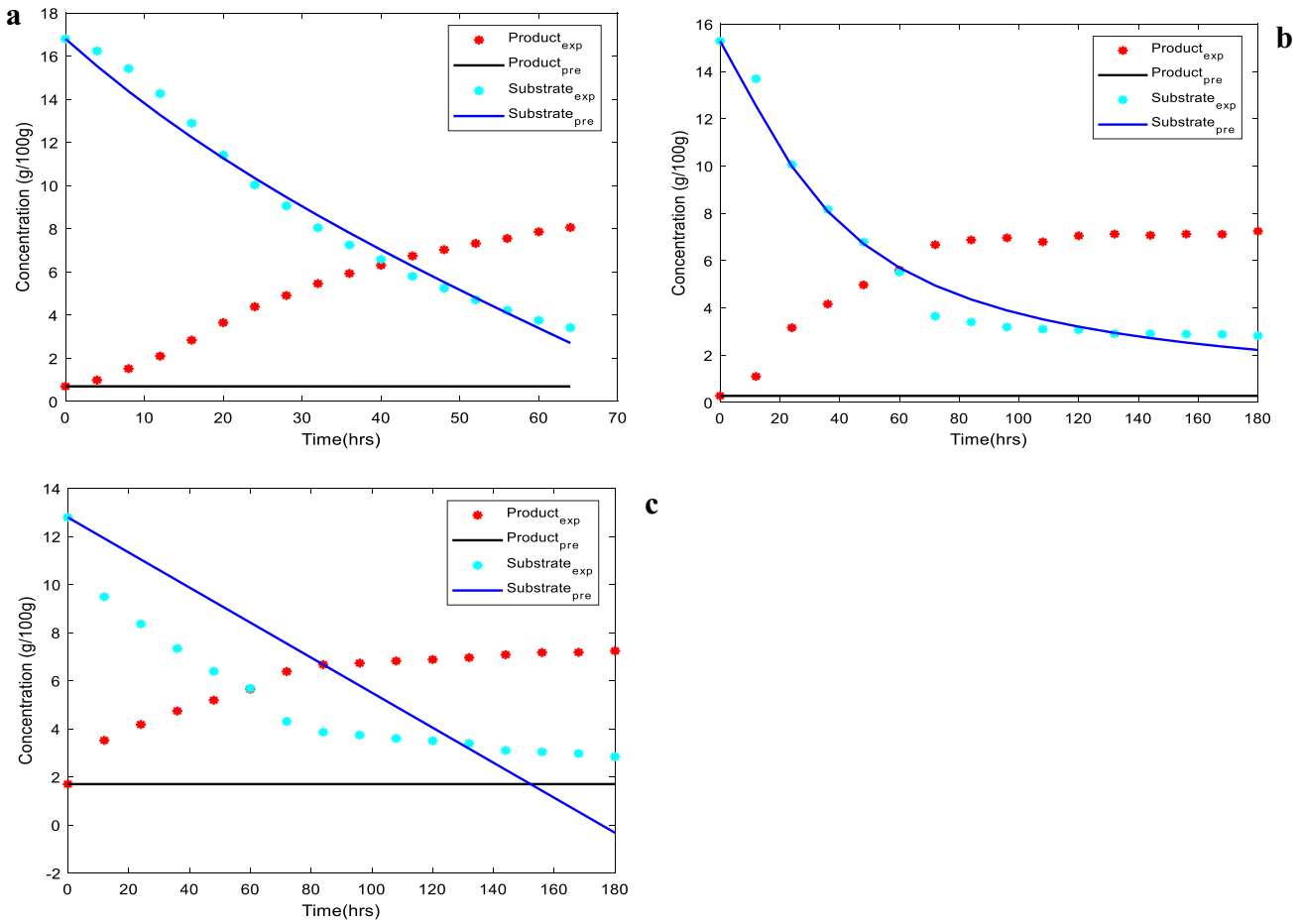

Fig. 5 Model fitting using one-dimensional substrate linear inhibition kinetics for fermentation of sorghum (**a**), Maize (**b**), and Cassava (**c**) extracts

Table 4 Estimation of kinetic constants and statistical validations for linear inhibition model

Model	Parameter estimates						Statistical validation		
	μ_{max}	K_s	Y_{PX}	Y_{XS}	M_s	K_{iS}	*RMSE*	χ^2	R^2
Batch 1: Sorghum extracts									
Linear	0.0010	0.0100	0.0100	9.9926	0.6789	1.2927	11.9689	576.5204	0.3110
Batch 2: Maize extracts									
Linear	0.001	0.000	0.000	0.006	14.698	4.688	16.613	1880.440	-0.621
Batch 3: Cassava extracts									
Linear	399.48	12.4839	176.955	-1.3895	-1.8490	0.3926	12.4839	176.9551	-1.3895

constants and statistical validation parameters that were utilized to fit the model. The exponential inhibition dynamic model showed a very high R^2 value (0.9967) and a very low RMSE value when fitted to sorghum extract data (Fig. 9a) (0.0565). The R^2 (0.8530) value of a model fitting the same product exponential inhibition dynamics with maize extract data (Fig. 9b) was extremely high. The same product exponential inhibition dynamic model was fitted to cassava extract data (Fig. 9c), yielding a high R^2 value (0.9845) and a low RMSE (0.0812).

Model fitting for the product sudden stop inhibition model with data from maize and cassava extracts is shown in Figure 10. Table 9 shows the calculated kinetic constants and statistical factors used to assess the fitting quality. Model fitting of the sudden stop inhibition model with cassava extract data (figure 10a) yielded a high R^2 value

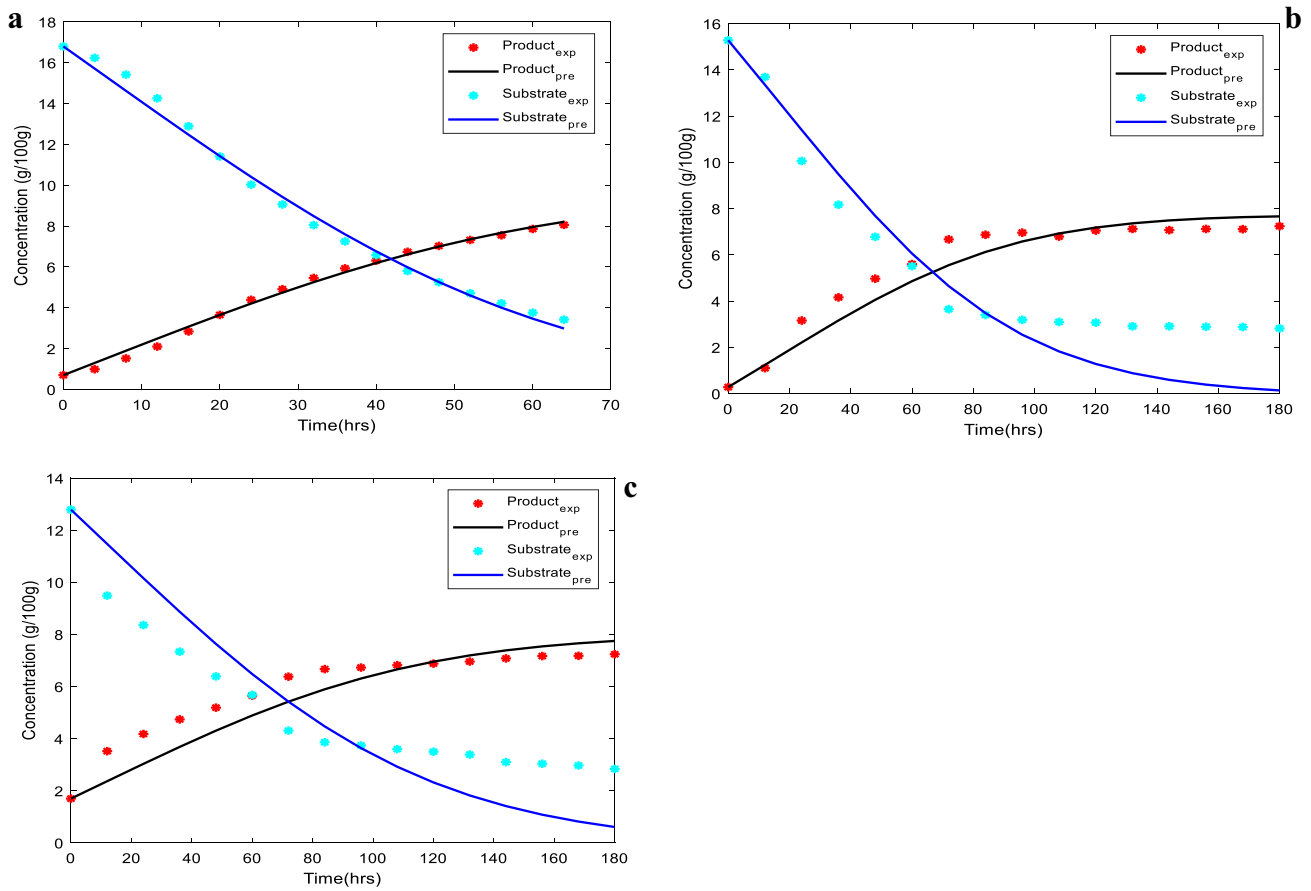

Fig. 6 Model fitting using one-dimensional substrate exponential inhibition kinetics for fermentation of sorghum (**a**), Maize (**b**), and Cassava (**c**) extracts

Table 5 Estimation of kinetic constants and statistical validations for exponential inhibition model

Model	Non-linear system estimation parameters values						Statistical validation parameters values		
	μ_{max}	K_s	Y_{PX}	Y_{XS}	M_s	K_{iS}	*RMSE*	χ^2	R^2
Batch 1: Sorghum extracts									
Exponential	0.0512	49.998	27.4032	0.0209	0.0100	0.0100	0.0956	0.5586	0.9945
Batch 2: Maize extracts									
Exponential	0.049	50.000	50.000	0.010	0.010	0.010	1.471	117.238	0.856
Batch 3: Cassava extracts									
Exponential	0.0387	50.0000	50.0000	0.0104	0.0100	0.0100	1.2976	25.0265	0.7516

(0.9874) and a low RMSE value (0.0661). Model fitting of the same model with maize extract data (figure 10b) also produced a good R^2 value (0.980).

4 Calculation of model fitness coefficient

The model fitness coefficients for the models included in the study were determined (Table 10) and dynamic models that best represented each set of process data were chosen. Sorghum extract data were best represented by a product exponential inhibition model (α = 0.4088), maize extract data by a product abrupt stop inhibition model (α = 0.6725), and cassava extract data by a product exponential model (α = 0.4417).

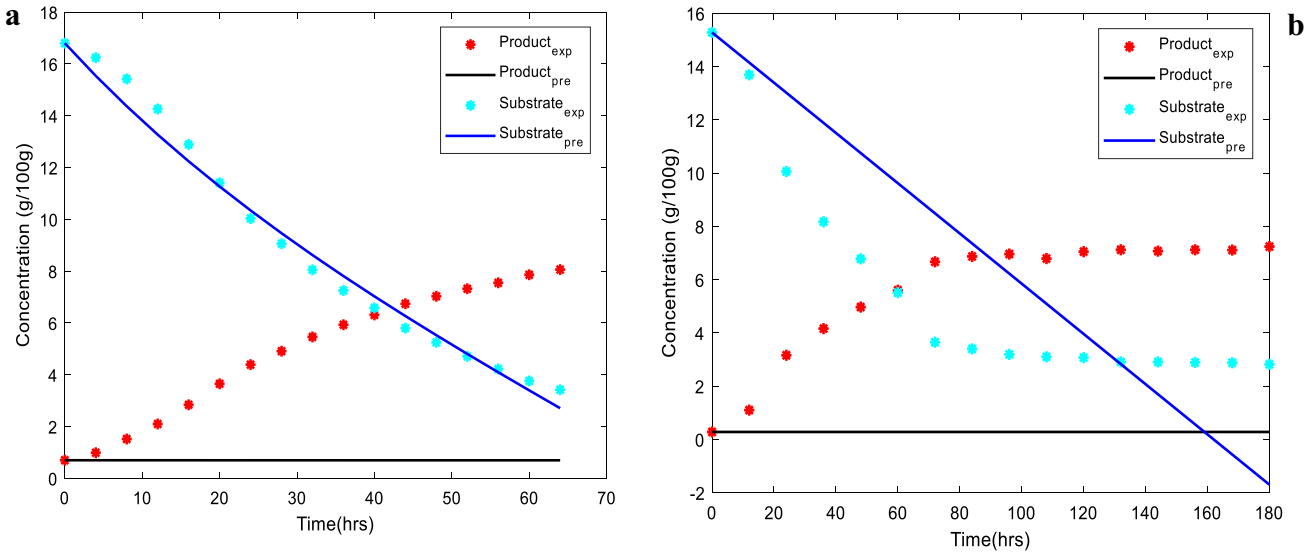

Fig. 7 Model fitting using one-dimensional substrate sudden-stop inhibition kinetics for fermentation of sorghum (**a**), Maize (**b**) extracts

Table 6 Estimation of kinetic constants and statistical validations for substrate sudden stop inhibition

Model	Non-linear system estimation parameters values						Statistical validation parameters values		
	μ_{max}	K_s	Y_{PX}	Y_{XS}	M_s	K_{iS}	*RMSE*	χ^2	R^2
Batch 1: Sorghum extracts									
Sudden stop	0.0010	0.0100	0.0100	9.9985	0.6789	0.7736	11.9689	576.5204	0.3110
Batch 2: Maize extracts									
Sudden stop	0.000	51.546	28.653	0.388	0.590	9.991	21.057	1869.142	-1.055

5 Visualizing inhibition effect and increase in yield

The effect of inhibition was visualized by displaying a visual representation of the substrate exponential inhibition model, the substrate linear inhibition model with the Monod model, as shown in this section. The effect of inhibition of the one-dimensional inhibition model that best described each substrate data; sorghum, maize, and cassava were simulated by plotting an inhibition curve and a no inhibition curve (Monod Model) on one graph as a graphical visualization of the two curves. The inhibition curve reveals overall substrate exhaustion. Figure 11a depicts a competitive inhibition. The No inhibition profile estimates a 20-h total substrate conversion time, which is significantly less than the inhibition curve's prediction (160 h). The sorghum extract was entirely exhausted within the stipulated time of substrate used for both models, resulting in a 74 percent increase in yield.

5.1 Exponential product inhibition effect with sorghum extract

The characteristics of sorghum extract data in Fig. 11b demonstrated a competitive inhibition since the inhibition curve reached a maximum concentration during product synthesis. The inhibition profile estimates a maximum product generation period of (180 h), whereas the No inhibition curve predicts a much shorter time (20 h).

5.2 Product substrate inhibition effect with maize extract:

The computed parameters of maize extract data in Fig. 12a depict a noncompetitive inhibition caused by incomplete substrate conversion. The No inhibition profile projected a 40-h total substrate conversion time, which is significantly less than the 180-h duration anticipated by the inhibition curve. The maize extract was not

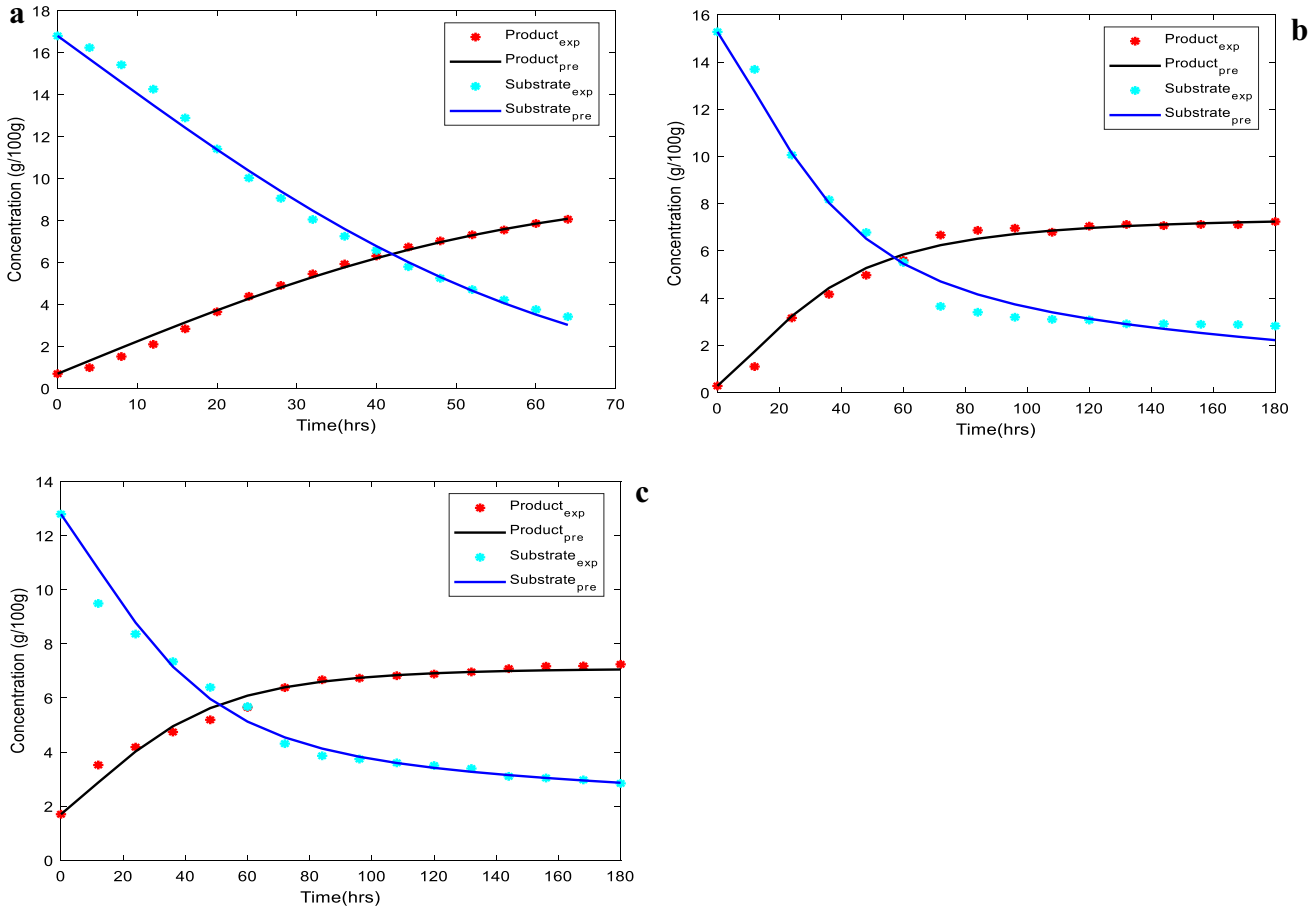

Fig. 8 Model fitting using one-dimensional product linear inhibition kinetics for fermentation of sorghum (**a**), Maize (**b**), and Cassava (**c**) extracts

Table 7 Estimation of kinetic constants and statistical validations for product linear inhibition

Model	Parameter estimates						Statistical characteristics		
	μ_{max}	K_s	Y_{PX}	Y_{XS}	M_s	K_{ip}	*RMSE*	χ^2	R^2
Batch 1: Sorghum Extracts									
Linear	0.0399	21.7613	18.3845	0.0334	0.0290	0.0411	0.0980	0.5787	0.9944
Batch 2: Maize Extracts									
Linear	0.237	48.026	12.235	0.050	0.010	0.134	0.153	1.252	0.9850
Batch 3: Cassava Extracts									
Linear	0.0726	6.4911	15.8288	0.0385	0.0106	0.1411	0.1077	0.5442	0.9794

depleted within the stipulated time of substrate used for both models, resulting in a projected yield increase of 27%.

The inhibition profile did not reach the maximum concentration in the product production, Fig. 12b, the estimated parameters of maize extract data, revealed a noncompetitive inhibition. When compared to the period indicated by the No inhibition curve, the inhibition profile revealed a much longer product production time (180 h).

5.3 Linear product inhibition effect with cassava extract

The inhibition profile achieved an incomplete substrate depletion, the predicted parameters of cassava extract data reflect a noncompetitive inhibition in Fig. 13a. The No inhibition profile, as expected, produced a complete substrate exhaustion time of 20 h, which is significantly less than the time predicted by the inhibition

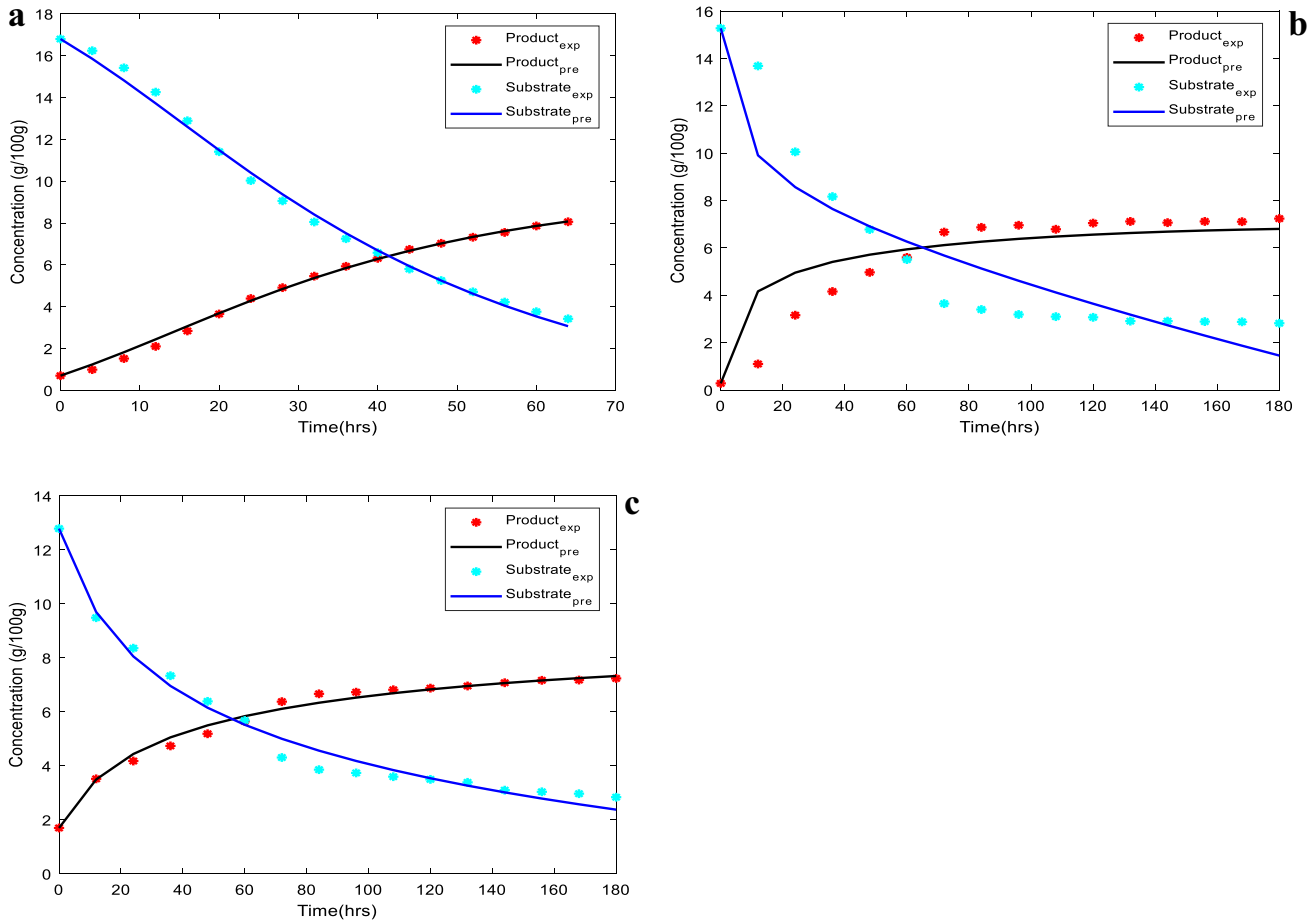

Fig. 9 Model fitting using one-dimensional product exponential inhibition kinetics for fermentation of sorghum (**a**), Maize (**b**), and Cassava (**c**) extracts

Table 8 Estimation of kinetic constants and statistical validations for product exponential inhibition

Model	Parameter estimates						Statistical characteristics		
	μ_{max}	K_s	Y_{PX}	Y_{XS}	M_s	K_{iP}	*RMSE*	χ^2	R^2
Batch 1: Sorghum extracts									
Exponential	0.1639	22.3715	4.0096	0.1697	0.0105	0.1623	0.0565	0.3490	0.9967
Batch 2: Maize extracts									
Exponential	2.273	47.611	31.257	0.025	0.085	0.865	1.508	9.580	0.8530
Batch 3: Cassava extracts									
Exponential	0.5966	17.8171	15.3383	0.0398	0.0104	0.6179	0.0812	0.5949	0.9845

curve (180 h). The extract, on the other hand, was not exhausted, and the calculated increase in yield was 25%.

The estimated parameters of cassava extract data demonstrated a noncompetitive inhibition in Fig. 13b. The inhibitory profile did not reach the maximal product formation concentration. In comparison to the much shorter anticipated time of the No inhibition curve, the inhibition profile revealed a much longer product production period of 180 h.

6 Control strategy for types of inhibitions

Control strategies that were proposed with the view to minimize inhibition are shown in Table 11 below:

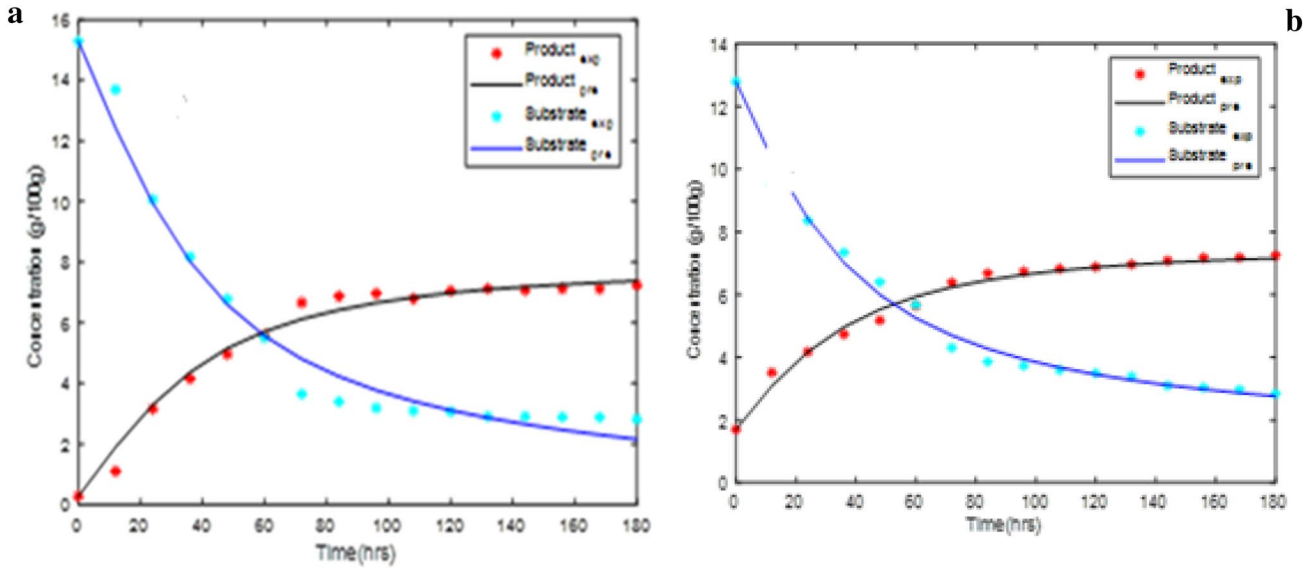

Fig. 10 Model fitting using one-dimensional product sudden stop inhibition kinetics for fermentation of (**a**), Maize (**b**), and Cassava extracts

Table 9 Estimation of kinetic constants and statistical validations for product sudden stop inhibition

Model	Parameter estimates						Statistical characteristics		
	μ_{max}	K_s	Y_{PX}	Y_{XS}	M_s	K_{iP}	*MSE*	χ^2	R^2
Batch 2: Maize Extracts									
Sudden stop	0.130	40.627	25.046	0.023	0.010	7.802	0.206	1.610	0.980
Batch 3: Cassava Extracts									
Sudden stop	0.1152	33.9245	32.8362	0.0178	0.0100	7.3787	0.0661	0.3630	0.9874

Table 10 Calculated model fitness coefficient (α) of determination value for both substrate and product inhibition models

Model	Substrate Inhibition α value	Product Inhibition α value	Substrate Inhibition α value	Product Inhibition α value	Substrate Inhibition α value	Product Inhibition α value
	Sorghum extract		Maize extracts		Cassava extracts	
Monod	0.6406	0.6585	78.703	79.129	22.3557	22.698
Linear	589.1783	0.6823	1898.674	11.235	191.8285	0.6916
Exponential	0.6597	0.4088	118.853	1.836	26.5725	0.4417
Sudden stop	589.1783	1.42	1892.254	0.6725	–	–

7 Discussions

To ensure large outputs of ethanol at the end of the fermentation, commercial ethanol batch fermentation requires a high concentration of substrate, typically between 18 and 22 percent (w/w) reducing sugars. Cell recycling has always been a concern for titters of ethanol up to 23 percent (v/v), and the fermentation duration is hampered, Basso et al. [19], Nogueira et al. [31] since yeast viability is vital to enable recycling. The occurrence of toxicity during ethanol fermentation renders the bioreactor useless since microbial cells are significantly impeded to the point where they can die in large numbers. Nonetheless, by investigating and understanding the roots of the inhibitory models, it is possible to pre-set substrate and product levels to avoid toxicity in the fermenter (Eqs. 2 to 7). Because the initial substrate concentration is between 18 and 22 percent (w/w) in total reducing sugar, a model fitness coefficient (α) of 0.045 or below is strongly recommended as the substrate inhibition constant to minimize toxicity for linear substrate inhibition. A model fitness coefficient (α) of 0.346 or lower is strongly advised to avoid toxicity for exponential substrate inhibition. Because

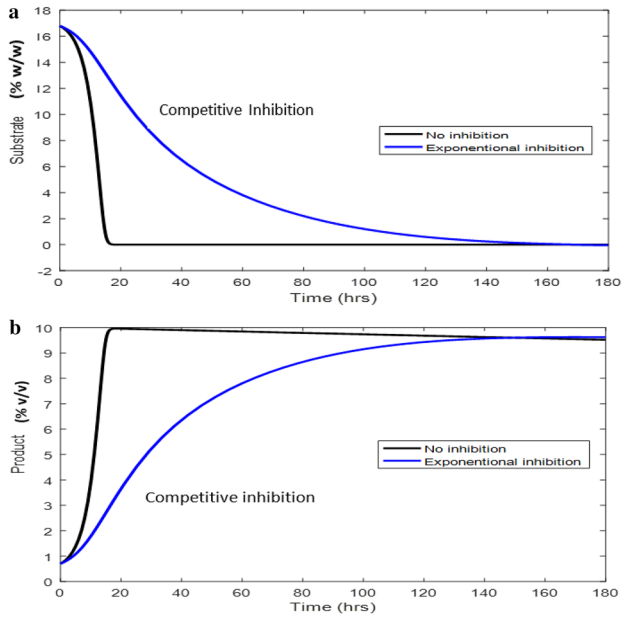

Fig. 11 **a** The plot of exponential product inhibition: competitive inhibition with sorghum, **b** The plot of exponential product inhibition effect with sorghum extract estimated parameters

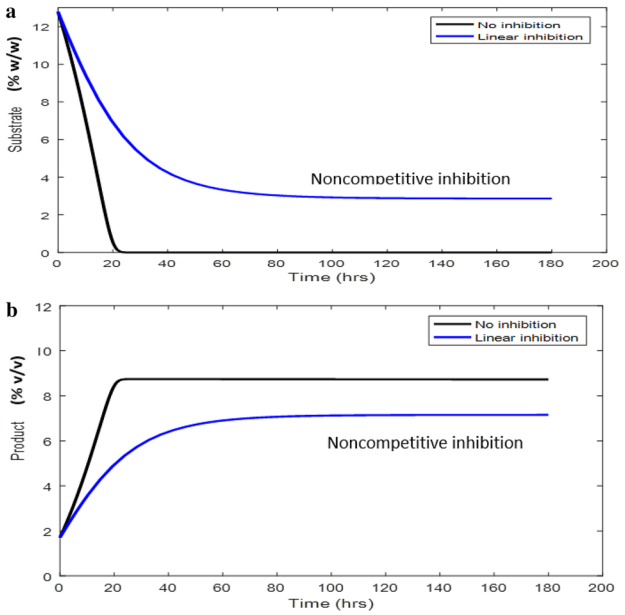

Fig. 13 **a** The plot of linear product inhibition effect with cassava extract estimated parameters, **b** The plot of linear product inhibition effect with cassava extract estimated parameters

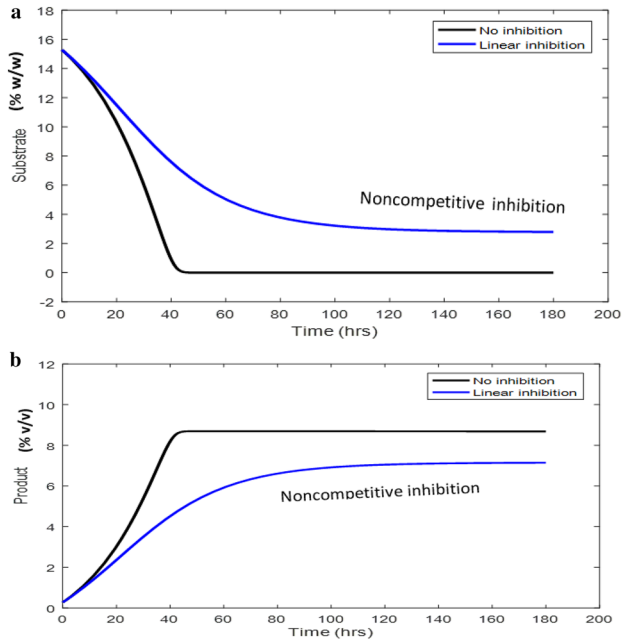

Fig. 12 (**a**) The plot of product substrate inhibition effect with maize extract estimated parameters, **b** The plot of linear product inhibition effect with maize extract estimated parameters

product titters can reach 23 percent (v/v), a model fitness coefficient (α) of 0.043 or below is strongly recommended as the product inhibition constant to minimize toxicity for a linear product inhibition. Because product titters can reach 23 percent (v/v), a model fitness coefficient (α) of 0.346 as the product inhibition constant is strongly recommended to avoid toxicity for an exponential product inhibition. It's worth noting that the linear inhibition pattern and the sudden stop inhibition pattern both produced equal model fitness coefficient results, implying that they're identical. Their physical meaning, on the other hand, differs, because a fermentation process with a linear pattern is expected to degrade slowly but surely towards toxicity, resulting in catastrophic cell death. The specific rate of microbial growth is reduced to zero as a result of this, a fermentation with a sudden stop pattern, on the other hand, is likely to swiftly degrade into toxicity, with a large number of microbial cells dying. In this instance, the specific rate of microbial growth is rapidly reduced to zero. The point here is that the linear inhibition pattern is considerably more dangerous to the process than the sudden stop inhibition pattern. The common denominator is that if allowed to, the process will stop with an excess of the substrate due to microorganisms' disinterest to continue converting the substrate into ethanol as a product. As a result, including both patterns at the same time for parameter estimation and model simulation is time-intensive unless their physical meanings are well understood and incorporated into the models. The findings of this study were found to agree with prior findings by other researchers, such as Chen and McDonald [32]. The relevance of the rate constant, K_i-, which originates from the substrate or product inhibition during ethanol fermentation cannot be overstated because it serves a dual role. The beginning substrate

Table 11 Control Strategy for Types of Inhibitions

Substrate	Inhibition model	Type of Inhibition	Control Strategy
Sorghum	Exponential product	Competitive inhibition	Operate at a high substrate concentration
Maize	Linear product	Noncompetitive inhibition	Operate at a low inhibitor concentration
Cassava	Linear product	Noncompetitive inhibition	Operate at a low inhibitor concentration

concentration and the desired product concentration at the end of the fermentation, the model can be utilized to control inhibition. Secondly, the rate constant, K_i., has the feature of being temperature-dependent. It can thus be modified using the Arrhenius equation to optimize the fermenter for the best temperature profile Petrou et al. [33].

8 Conclusion

The study was prompted by the fact that the existing global economy relies heavily on fossil fuels for energy to efficiently power both industrial and home operations. While fossil fuel supplies are finite, and their exploitation over time exacerbates the negative impacts of high greenhouse gas emissions, bioethanol is slowly but steadily becoming more widely used in the energy business to help preserve our society's energy supply. This research has provided unique contributions that have yet to be implemented in the biochemical process sector. This study demonstrated that a combination of mechanical translations of fermentation inhibitions into the physical environment of an industrial fermentation process via mathematical models resulted in both qualitative and quantitative interpretation of the results. The goal of this project was to create a framework for one-dimensional substrate and product inhibition to better understand how sorghum, maize, and cassava extracts behaved during the fermentation process. Two inhibition geometries for Substrate and Product were created, and by changing the Monod equation, a total of six (6) one-dimensional inhibition equations were generated.

The use of a non-convoluted recombination process incorporating the Monod equation, two inhibitors, and three inhibition patterns made this achievable. For a system of three states involving Substrate, Product, and Biomass, stoichiometric biochemical reaction schemes within the fermenter was established, as well as a system of dynamic equations for a batch ethanol fermentation process. This showed a material balance that described the fermentation processes using first-order differential and algebraic equations. Models of the fermenter's behavior and parameters about the feedstock were built with the help of the construction of the fermenter. This allowed data to be extracted on the quality of each feedstock (sorghum, maize, or cassava). The values of the statistical model fitness coefficients were used to determine the best performing dynamic model for each feedstock, and the best fitting model with the lowest value of the model fitness coefficient was chosen for each feedstock. In summary, Product Exponential inhibition emerged as the best one-dimensional inhibition models that best-described sorghum data ($\alpha = 0.0859$), Product Linear and Product Sudden stop inhibitions equally appeared as the best performed one-dimensional inhibition models that best-described maize extract data ($\alpha = 2.3786$ and $\alpha = 2.3786$ respectively) and Product Linear and Product Sudden stop inhibitions equally came out as the best one-dimensional inhibition models that described cassava extract data ($\alpha = 2.0628$ and.

$\alpha = 2.0628$ respectively). Competitive inhibition was seen in sorghum, while non-competitive inhibition was observed in maize and cassava. The most appropriate control approach necessary to decrease inhibition was qualitatively examined in terms of control strategies. The study provided a library of one-dimensional inhibitory kinetics models that are very dependable in the mitigation of inhibitions for ethanol fermentation, it has the potential to improve fermenter design. It has cleared the path for newer fermentation technology improvements.

Acknowledgements The authors express gratitude to the Department of Chemical Engineering, Kwame Nkrumah University of Science and Technology (KNUST) Kumasi Ghana. Our sincere gratitude also goes to Mr. Jesse Essuman Johnson and Miss Emilia Nyumuteye for their invaluable contributions during the revision stages of the manuscript.

Declarations

Conflict of interest The authors declare that they have NO affiliations with or involvement in any organization or entity with any financial interest, or non-financial interest in the subject matter or materials discussed in this manuscript.

References

1. Vohra M, Manwarb J, Manmodec R, Padgilwarb S, Patila S (2014) Bioethanol production: feedstock and current technologies. J Environ Chem Eng. https://doi.org/10.1016/j.jece.2013.10.013
2. Choi Y, Rayl J, Tammineedi C, Brownson JRS (2011) PV Analyst: coupling ArcGIS with TRNSYS to assess distributed photovoltaic potential in urban areas. Sol Energy 85(11):2924–2939. https://doi.org/10.1016/j.solener.2011.08.034
3. Pulidindi IN, Kimchi BB, Gedanken A (2014) Can cellulose be a sustainable feedstock for bioethanol production? Renew Energy 71:77–80. https://doi.org/10.1016/j.renene.2014.05.032
4. Marshall E, Mejia D (2012) Traditional fermented food and beverages for improved livelihoods. United Nations (FAO), Rome Italy
5. Harde SM, Bankar SB, Ojamo H, Granstrom T, Singhal RS et al (2014) Continuous lignocellulosic ethanol production using Coleus forskohlii root hydrolysate. Fuel 126:77–84. https://doi.org/10.1155/2014/532852
6. Chisti Y (2007) Biodiesel from microalgae: a research review paper. Biotechnol Adv 25:294–306. https://doi.org/10.1016/j.biotechadv.2007.02.001
7. Goh CSK, Lee KTA (2010) Visionary and conceptual macroalgae-based third-generation bioethanol (TGB) biorefinery in Sabah Malaysia as an underlay for renewable and sustainable development. Renew Sustain Energy Rev 14(2):842–848
8. Alriksson B (2006) Ethanol from lignocellulose: Alkali detoxification of dilute-acid spruce hydrolysates. Dissertation, Karlstad University
9. Alford JS (2006) Bioprocess Control: Advances and challenges. Comput Chem Eng 30:1464–1475. https://doi.org/10.1016/j.compchemeng.2006.05.039
10. Asiedu NY, Abunde NF, Addo A (2016) Modeling and simulation of substrate and product inhibitions of fermentation of cassava (Manihot Esculenta) extract. Ind Biotechnol. https://doi.org/10.1089/ind.2016.0001
11. Han K, Levenspiel O (1987) Extended monod kinetics for substrate, product, and cell inhibition. Biotechnol Bioeng. https://doi.org/10.1002/bit.260320404
12. Palsson B, Oberhardt MA, Papin JA (2009) (2009) Applications of genome-scale metabolic reconstructions. Mol Syst Biol 5:320. https://doi.org/10.1038/msb.2009.77
13. Brenner S (2010) Sequences and consequences. Philos T Roy Soc B 365:207–212. https://doi.org/10.1098/rstb.2009.0221
14. Schoneberger JC, Arellano-Garcia H, Wozny G (2010) Local optima in model-based optimal experimental designs. Ind Eng Chem Res 49(20):10059–10073. https://doi.org/10.1021/ie9016094
15. Boer EPJ, Hendrix EMP (2000) Global optimization problems in optimal design of experiments in regression models. J Global Opt 18:385–398. https://doi.org/10.1023/A:1026552318150
16. Yu L, Wensel PC, Ma J, Chen S (2013) Mathematical modeling in Anaerobic Digestion (AD). J Bioremed Biodeg. https://doi.org/10.4172/2155-6199.S4-003
17. Ming D, Glasser D, Hildebrandt D, Glasser B, Metzger M (2016) Attainable Region Theory: An introduction to choosing an optimal reactor. Wiley
18. Abunde NF, Asiedu N, Addo A (2016) Dynamics of inhibition patterns during fermentation processes-Zea Mays and Sorghum Bicolor: Case study. Int J Ind Chem 8:91–99. https://doi.org/10.1007/s40090-016-0105-9
19. Harmelen FV, Lifschitz V, Porter B (2008) Handbook of knowledge representation. Elsevier
20. Kristensen JB, Felby C, Jorgensen H (2009) Yield-determining factors in high-solids enzymatic hydrolysis of lignocellulose. Biotechnol Biofuels 2:11. https://doi.org/10.1186/1754-6834-2-11
21. Kaparaju P, Serrano M, Thomsen BA, Kongjan P, Angelidaki I (2009) Bioethanol, biohydrogen, and biogas production from wheat straw in a bio-refinery concept. Biores Technol 100:2562–3256. https://doi.org/10.1016/j.biortech.2008.11.011
22. Basso LC, Basso TO, Rocha SN (2011) Ethanol production in Brazil: The industrial process and its impact on yeast fermentation. Biofuel Production- Recent Developments and Prospects. IntechOpen
23. Stambaugh R, Post D (1966) Substrate and product inhibition of rabbit muscle lactic dehydrogenase Heart (H4) and Muscle (M4) Isozymes. J Biol Chem 241(7):1462–1467. https://doi.org/10.1016/S0021-9258(18)96733-5
24. Monod JL (1942) Research on the growth of bacterial cultures. Annual Rev Microbiol 3:371–394
25. Hinshelwood CN (1946) Chemical kinetics of the bacterial cell. Oxford Clarendon Press
26. Aiba S, Shoda M, Nagatani M (1968) Kinetics of product inhibition in alcohol fermentation. Biotechnol Bioeng 10(6):845–864. https://doi.org/10.1002/bit.260100610
27. Ghose TK, Tyasi RD (1979) Rapid ethanol fermentation and cellulose hydrolysate: product and substrate inhibition and optimization of fermenter design. Biotechnol Bioeng. https://doi.org/10.1002/bit.260210808
28. Bastin G, Dochain D (1990) Process measurement and control: Online estimation and adaptive control of bioreactors. Vol 1,(ed 1) New York (USA)
29. Hahn GJ (1973) Coefficient of determination exposed. Chemical Technology. American Chemical Society (USA)
30. Huangn LS, Chei J (2008) Analysis of variance: Coefficient of determination and F-test for local polynomial regression. Annal Stat 36(5):2085–2109
31. Cameron AL, Windmeijer FAG (1996) R-Squared measures for count data regression models with applications to health care utilization. J Bus Econ Stat 14(2):209–220. https://doi.org/10.2307/1392433
32. Contois DE (1959) Kinetics of bacterial growth: relationship between population density and specific growth rate of continuous cultures. J Gen Microbiol 21:40–50. https://doi.org/10.1099/00221287-21-1-40
33. Boekhorst RH, Ogilvie JR, Pos J (1981) An overview of current simulation models for anaerobic digesters. National Recreation and Park Association (USA)
34. Pfeffer JT (1974) Temperature effects on anaerobic fermentation of domestic refuse. Biotechnol Bioeng 16:771–787. https://doi.org/10.1002/bit.260160607
35. Nogueira LAH, Capaz RS (2013) Biofuels in Brazil: evolution, achievements, and perspectives on food security. Glob Food Sec 2(2):117–125. https://doi.org/10.1016/j.gfs.2013.04.001
36. Chen CI, McDonald KA (1990) Oscillatory behavior of Saccharomyces cerevisiae in continuous culture: I. Effects of pH and nitrogen levels. Biotechnol Bioeng. https://doi.org/10.1002/bit.260360104
37. Petrou AL, Roula M, Tampouris K (2002) The use of the Arrhenius equation in the study of deterioration and of cooking of foods-some scientific and pedagogic aspects. Chem Edu: Res Pract Eur 3(1):87–97